

Lateral earth pressure at rest in response to pore water pressure increases in saturated sand

Tzou-Shin Ueng¹, G.-L. Huang¹, Y.-C. Tsai¹, and L. Ge¹

¹ Department of Civil Engineering, National Taiwan University, Taipei, 10617, Taiwan.

ABSTRACT

This paper presents the test results of lateral pressures of a saturated fine silica sand column in response to pore water pressure changes. The pore water pressure increases were induced by: (1) an upward flow gradient and (2) vibrations at the bottom of the sand column. The lateral earth pressures at various depths were measured within the sand specimen and the pore water pressures were measured at the same depths of the earth pressure measurements. The pore pressures and lateral pressures were recorded continuously during changes of pore water pressures. The test results showed that, due to the particle interlocking, at the beginning of pore water pressure increase, the total lateral pressure increased by the same amount of the pore pressure generation; that is, the effective lateral pressure remained the same initial value while the effective vertical stress reduced due to pore pressure increases. As a result, K_0 increases to values even larger than 1.0. This sand particle interlocking started to diminish as the pore pressure ratio r_u reached a value of around 0.2~0.5 or at $K_0 = 0.6$ ~0.7. The effects of aging on the lateral earth pressure at rest were also studied.

Keywords: earth pressure at rest; pore water pressure; saturated sand; particle interlocking

1 INTRODUCTION

The backfill materials behind the waterfront retaining facilities in coastal regions and port areas are often backfilled with sandy soils mostly in a saturated condition. Therefore, variations of pore water pressure within these backfill materials would have a great impact on the lateral thrust on the retaining structures. During earthquakes, combination of lateral earth pressure and the pore water pressure of the backfill soil could cause excessive deflections resulting in failures of the retaining structures. However, the coupling effect of the change of pore water pressure on the lateral earth pressure was seldom considered in computations of the lateral forces acting on the retaining structures.

The total lateral pressure acting on a retaining wall with a saturated backfill is conventionally obtained as shown in Fig. 1 for a hydrostatic condition by calculating the effective lateral earth pressures according to the earth pressure theory plus the water pressures at different depths of the retaining wall, i.e.,

$$\sigma'_h = K\sigma'_v = K(\sigma_v - u) \quad (1)$$

$$\sigma_h = \sigma'_h + u \quad (2)$$

where σ'_h = effective lateral stress

σ'_v = effective vertical stress

K = coefficient of earth pressure

σ_h = total lateral stress

σ_v = total vertical stress = $\gamma_{sat} z$

u = pore water pressure = $\gamma_w z_w$

γ_{sat} , γ_w = unit weights of backfill soil and water

z , z_w = depths of backfill soil and water

It can be seen that the water pressure changes would affect the vertical effective stresses σ'_v and in turn the lateral effective stresses σ'_h according to the coefficient of earth pressure K which is usually assumed a constant value. However, some field and laboratory evidences showed that the value of K may change in response to the changes of pore water pressure, especially induced by vibration loadings, and the lateral pressure could be quite different from those calculated conventionally, e.g., Chen (2013), Dewoolkar et al. (2001).

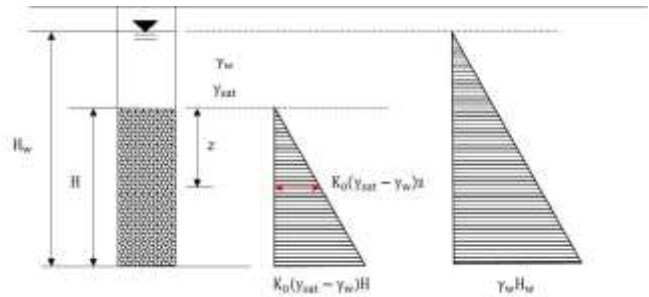


Fig. 1. Lateral earth pressure on a retaining wall.

In this study, experiments were conducted with earth pressure transducers placed at different depths in a saturated sand column to measure the changes of lateral earth pressure in response to pore water pressure generations due to either upward flows or vibrations under the condition of no lateral displacement, i.e., a K_0 condition, to evaluate the influence of pore water pressure changes on the behavior of sand particles and its effect on the lateral earth pressure.

2 EXPERIMENT SETUP AND SPECIMEN PREPARATION

The experimental system shown schematically in Fig. 2 includes a 10-mm thick transparent acrylic tube with 100 mm in inner diameter and 1000 mm in length with an overflow device on top, a constant head water supply system, and an instrumentation and data acquisition system for continuous measurements of water pressures, soil pressures, flow rate, and vibrations during the tests.

Three water pressure transducers, P1, P2, and P3 were installed on the wall of the acrylic tube at heights of 450 mm, 350 mm and 200 mm, respectively, from the bottom of the sand column, followed by slowly introducing de-aired water from the bottom of the sand column. The installed water pressure transducers were soaked in the de-aired water for 24 hours prior to preparation of the sand specimen. The earth pressure transducers, EPs, were first glued on a thin plastic sheet. Fish wires were then attached on the plastic sheet and the lateral earth pressure transducer with the sensing surface facing horizontally was placed at the desired location by adjusting the lengths of the wires prior to specimen preparation. The vertical earth pressure gages were placed at the desired depths during specimen preparation. An effort was made to ensure the sensor facing vertically during the experiment.

Fine Vietnam silica sand with a specific gravity $G_s = 2.65$, mean grain size $D_{50} = 0.3$ mm, maximum void ratio $e_{\max} = 0.906$, and minimum void ratio $e_{\min} = 0.631$ was used for the saturated sand specimen with a unit weight of 18.85 kN/m^3 in this study. The friction angle of this saturated sand $\phi' = 34^\circ$ according to the results of direct shear tests. A sand column of 500 and 600 mm in height was prepared in 10 and 12 layers by wet sedimentation method into the acrylic tube for the upward flow tests and the vibration tests, respectively. The thickness of each layer after preparation was 50 mm. Detailed descriptions of the experiment system and specimen preparation are given in Huang (2016) and Tsai (2017).

3 TEST PROGRAM

Pore water pressure changes in the sand specimen were induced by either upward seepage flows or vibrations with a frequency of about 4-5 Hz applied at the base of the acrylic tube. The flow velocity increased from 0 to 0.05 cm/s and reduced back down to 0 cm/s for a test cycle. The pore pressure ratio r_u reached around 0.7~0.8, which was very close to the state of sand boiling. The earth pressures and water pressures were measured at depths of 50 and 150 mm below the sand surface during the flow cycles. Two tests were performed for each depth of measurement.

Vibrations were applied at the base of the acrylic tube to induce the pore water pressure generations. For

most of the cases under vibrations, liquefaction occurred when pore water pressures reached the total stress, i.e., $r_u = 1.0$. The earth pressures and water pressures were measured at depths of 150 and 250 mm below the sand surface during the vibration applications. The vibrations were applied immediately, 24 hours and 48 hours after the completion of specimen preparation to evaluation the aging effect on the lateral pressure. Table 1 shows the schedule of the tests performed for pore water pressure changes under vibrations.

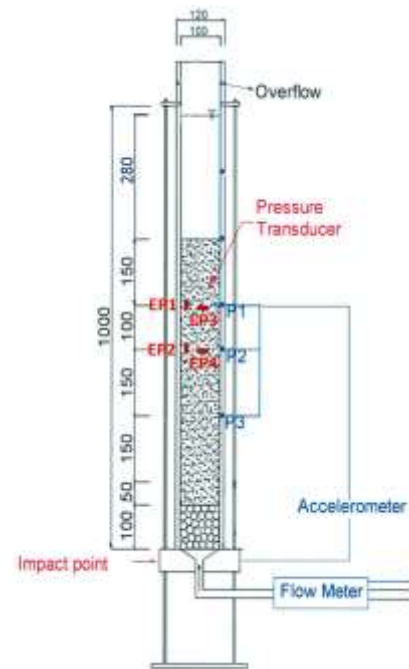


Fig. 2. Sand column and testing setup.

Table 1. Tests under vibration applications

Test No.	Measuring depths (mm)	Time after preparation (hr)
VTI0-1	150	0
VTI0-2	250	0
VTI24-1	150	24
VTI24-2	250	24
VTI48-1	150	48
VTI48-2	250	48
VTII0	150, 250	0
VTII24	150, 250	24
VTII48	150, 250	48

4 TEST RESULTS

The stresses measured by the earth pressure transducers in the experiment were the total stresses. The effective stresses were obtained by deducting the measured water pressures from the total stresses. Since there was little lateral deformation of the sand specimen inside the rigid acrylic tube, the measured lateral earth pressures are considered as the earth pressure at rest.

4.1 Lateral earth pressures under upward flows

The effective vertical earth pressures σ'_v measured at the depths of 50 and 150 mm after specimen preparation were 0.43 kPa and 1.45 kPa, respectively. They are close to the calculated values of 0.45 and 1.36 kPa, respectively, based on the unit weight of the soil specimen. Meanwhile, the measured effective lateral earth pressures σ'_h are 0.186 and 0.695 kPa, respectively, at the depths of 50 and 150 mm. The average coefficient of earth pressure at rest K_0 is 0.46. This is very close to the value of 0.44 computed according to the commonly used Eq. (3) proposed by Jaky (1944).

$$K_0 = 1 - \sin \phi' \quad (3)$$

Figure 3 shows results of the measured σ'_h versus r_u induced by the upward flows. It indicates that there was a very small change of σ'_h at the beginning of water pressure increasing up to $r_u \approx 0.3$; more significant decrease of σ'_h occurred at a higher r_u with a larger flow velocity. Because of the friction between the sand and acrylic tube wall, the total vertical stress in the sand specimen increased with increasing flow velocity. K_0 values calculated based on the measured lateral and vertical pressures are shown in Fig. 4. It can be seen K_0 increased from 0.45 to above 0.6 as pore water pressure increases.

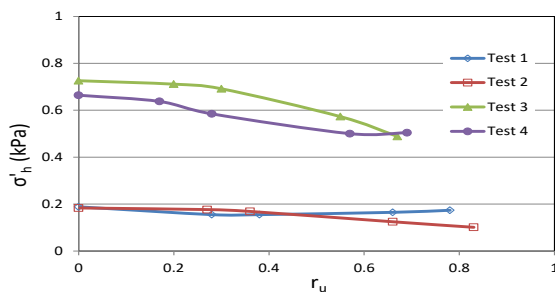


Fig. 3. Effective lateral pressures versus r_u .

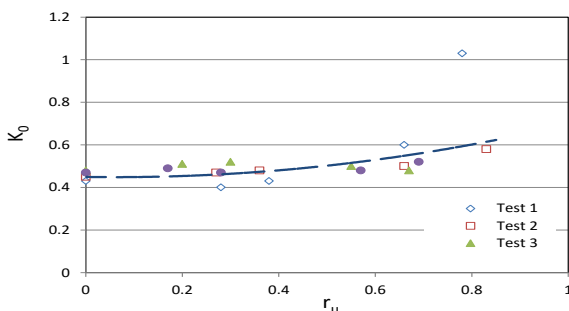


Fig. 4. K_0 versus r_u .

4.2 Lateral earth pressures under vibrations

In these experiments, K_0 were calculated according to the measured earth pressures and water pressures during and after specimen preparation. It was found that K_0 values were generally in the range between 0.4 and

0.44. This is close to the calculated value 0.44 according to Eq. (3). The measured vertical stresses at various depths were also in agreement with the calculated values based on the unit weight of the sand specimen.

Figure 5 shows typical time histories of measured vertical and horizontal earth pressures under vibrations at a depth of 150 mm (Test VTIO-1). It can be seen that σ'_v remained about the same initial value except a sudden pulse response at the beginning of the vibration application. On the other hand, σ'_h increased in response to the vibrations and could reach a value higher than the total vertical stress.

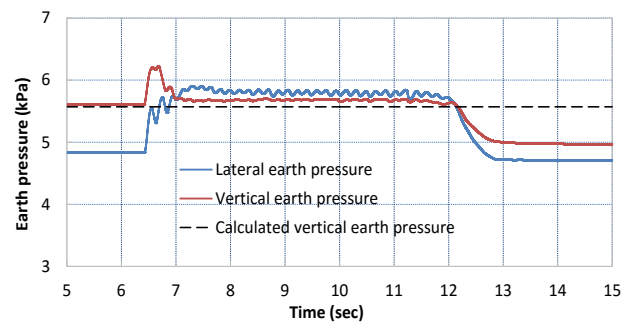


Fig. 5. Time histories of earth pressures under vibrations (VTIO-1).

The change of σ'_h during vibration Test VTIO-1 is also plotted alongside with the change of water pressure Δu as shown in Fig. 6. It shows that, at the beginning of vibration, σ'_h increased simultaneously with the pore water pressure increase. The changes of both σ'_h and water pressure are about the same until Δu reached about 0.9 kPa (time ≈ 7 s on Fig. 6). That is, σ'_h did not change during this period while σ'_v reduced because of pore pressure generation. This phenomenon is considered due to the effect of sand particle interlocking. The horizontal contact stresses between sand grains remain intact regardless of reduction of the vertical contact stresses. As a result, K_0 could even increase to more than 1.0. Fig. 7 shows variations of K_0 value during Test VTIO-2.

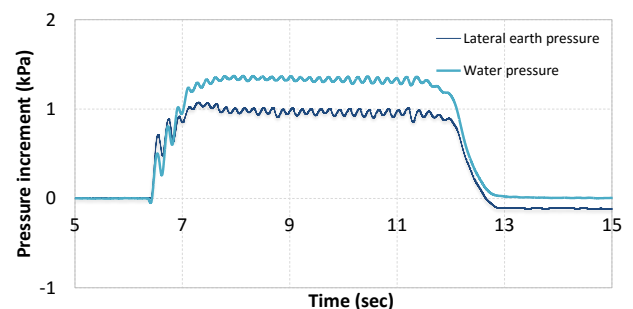


Fig. 6. Comparison of changes of σ'_h versus Δu (VTIO-1).

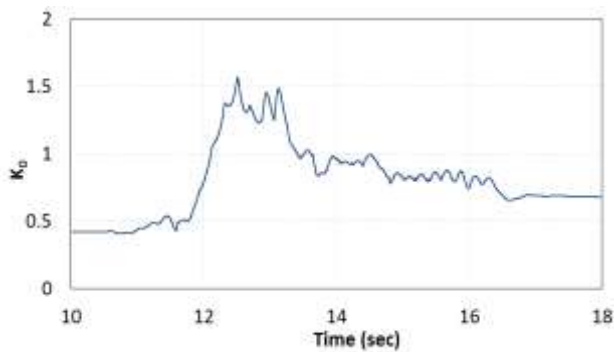


Fig. 7. K_0 time history in Test VT10-2.

According to the test results in this study, the interlocking effect started to diminish at $r_u \approx 0.2 \sim 0.5$ or $K_0 = 0.6 \sim 0.7$ when the contacts between sand grains weakened due to the higher pore water pressure and vibration disturbance. At this stage, the increase of σ_h was less than that of water pressure. σ_h , and consequently K_0 , decreased when the soil approached liquefaction.

The aging effect on K_0 was also evaluated by measuring the changes of σ_h and σ_v after completion of specimen preparation. Fig. 8 shows changes of K_0 values from 0 to 48 hours after completion of specimen preparation before vibration applications. The K_0 values increased from approximately 0.4 immediately after completion of specimen preparation to around 0.5 and 0.6 after 24 and 48 hours, respectively.

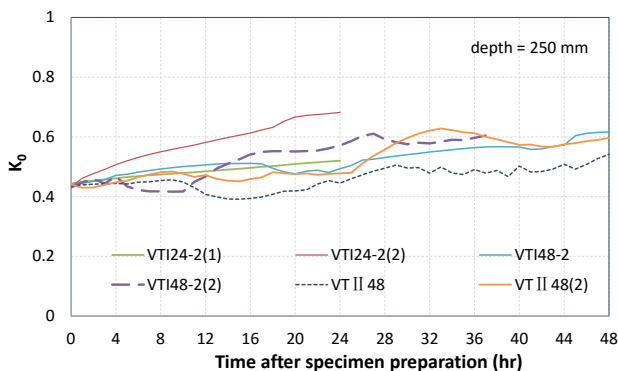


Fig. 8. K_0 versus time after specimen preparation

It was found in this study that there was only a slight increase of particle interlocking due to aging effect in regard to the lateral earth pressure under vibrations.

Because of the effect of particle interlocking, the total lateral earth pressure on a water front retaining structure with a saturated granular backfill under earthquake shakings can exceed the value calculated according to Eqs. (1) and (2). It could even possibly

rise to a value higher than the total vertical overburden pressure. This leads to a higher lateral thrust force on the retaining structure than that computed according to the ordinary design method. Based on the test results obtained in this study, owing to the pore water pressure generation and interlocking effect, an increment of 15 to 20%, of the original static total lateral force could possibly act on the retaining structure in addition to the dynamic forces induced by the ground shakings.

5 CONCLUSIONS

The experimental results in this study show that the lateral earth pressure rises with the water pressure generation simultaneously under upward flow or vibrations. Thus, the effective lateral earth pressure does not change at the beginning of water pressure increase. This may be due to the interlocking between sand grains during pore water pressure changes. With the vertical effective stress decreasing due to the water pressure generation, K_0 would accordingly increase. It can possibly be more than 1.0. The lateral earth pressure would therefore increase more than the values calculated according to the conventional earth pressure theory and may possibly exceed the total overburden pressure. The sand particle interlocking started to diminish as r_u reached a value of around 0.2~0.5 or at $K_0 = 0.6 \sim 0.7$. In addition, K_0 increases from about 0.4 to 0.5~0.6 during the period of 24 and 48 hours after completion of specimen preparation due to the aging effect.

REFERENCES

- Chen, C. H. (2013). Shaking Table Tests on Soil-Pile-Structure Interaction—Results of Earth Pressure Measurements, NCREC, Taiwan (unpublished). Canadian Geotechnical Journal, 1(1), 16-26.
- Dewoolkar, M. M., Ko, H. Y. and Pak, Y. S. (2001). Seismic behavior of cantilever retaining walls with liquefiable backfills. Journal of Geotechnical and Geoenvironmental Engineering, ASCE, 127(5), 424-435.
- Huang, G. L. (2016). The Effect of Pore Pressure Change on Lateral Earth Pressure at Rest in Saturated Sand, M. S. thesis, Department of Civil Engineering, National Taiwan University, Taipei, Taiwan.
- Jaky, J. (1944). The coefficient of earth pressure at rest. Journal of the Hungarian Society of Architects and Engineers, 25, 355-358.
- Tsai, Y. C. (2017). Effect of Vibration-induced Water Pressure Generation on Lateral Earth Pressure at Rest in Saturated Sand, M. S. thesis, Department of Civil Engineering, National Taiwan University, Taipei, Taiwan.